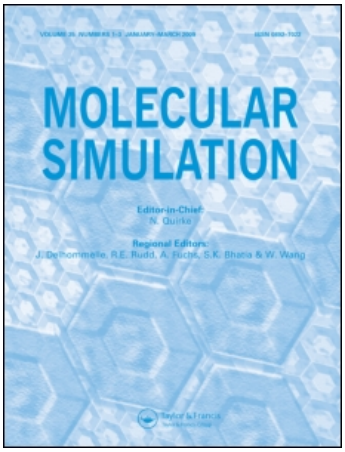

Molecular Simulation
Publication details, including instructions for authors and subscription information:
http://www.informaworld.com/smpp/title~content=t713644482

The effect of reciprocal-space sampling and basis set quality on the calculated conductance of a molecular junction

R. C. Hoft[a]; M. J. Ford[a]; M. B. Cortie[a]
[a] Institute for Nanoscale Technology, University of Technology Sydney, Broadway, NSW, Australia

Online publication date: 27 July 2010

To cite this Article Hoft, R. C. , Ford, M. J. and Cortie, M. B.(2007) 'The effect of reciprocal-space sampling and basis set quality on the calculated conductance of a molecular junction', Molecular Simulation, 33: 11, 897 — 904
To link to this Article: DOI: 10.1080/08927020701435811
URL: http://dx.doi.org/10.1080/08927020701435811

Molecular Simulation, Vol. 33, No. 11, September 2007, 897–904

Taylor & Francis
Taylor & Francis Group

The effect of reciprocal-space sampling and basis set quality on the calculated conductance of a molecular junction

R. C. HOFT, M. J. FORD* and M. B. CORTIE

Institute for Nanoscale Technology, University of Technology Sydney, P.O. Box 123, Broadway, NSW 2007, Australia

(Received March 2007; in final form May 2007)

We perform density functional theory and non-equilibrium Green's function calculations of the conductance of a gold wire and a 1,4-phenylenedimethanethiol (XYL) molecule adsorbed between Au(111) electrodes using the TranSIESTA software package. The effect of varying different computational parameters is investigated. We find that the conductance is more sensitive to the reciprocal-space sampling grid than the quality of the basis set employed. The conductance can vary up to a factor of five as a result of the choice of computational parameters. We report a set of computational parameters that yields a well-converged conductance value.

Keywords: Molecular conductance; Molecular junction; Density Functional Theory; Non-equilibrium Green's function

PACS numbers: 73.63.-b; 73.40.Gk; 85.35.-p

1. Introduction

Molecular electronics is an active area of research with the eventual goal of building an electronic device with molecules as its active components [1]. Recent advances in both the experimental [2] and theoretical [3] realm concerning the conductance of individual molecules are bringing this goal closer to reality. However, a cause for concern is the large discrepancies that still exist between available data, both experimental and theoretical [4].

Molecules with thiol endgroups form strong bonds to Au(111) substrates and their formation of self-assembled monolayers (SAMs) is well studied [5]. For this reason, the thiol "alligator-clip" is commonly used in molecular conduction experiments. Many experiments probe the current–voltage response of a SAM using scanning tunneling spectroscopy (STS). Here, the current between an STM tip and substrate under an applied bias [6–14] at fixed tip height is measured. Among other experimental tools are mechanical break junctions [15–17] and atomic force microscopes (AFM) with a conducting tip [18]. Various authors have claimed to measure the $i(V)$ response of an individual molecule, e.g. [13,14,16,18].

Theoretically, experimental setups are usually approximated by two semi-infinite Au(111) slabs sandwiching the molecule under study. The theoretical determination of the current passing between these electrodes is complicated beyond the usual electronic structure calculation by the fact that the system, under an applied bias between the electrodes, is not in equilibrium. Density functional theory is typically used as the starting point for conductance calculations, and yields the equilibrium electronic structure of the molecule plus electrodes. The transmission function and hence current is then calculated according to the non-equilibrium Green's functions method (NEGF). This combination is now an established tool for *ab initio* molecular transport calculations (see, for example, a recent review by Lindsay and Ratner [19]). The choice of basis functions and sampling of the Brillouin zone are critical factors that can affect the result when calculating the electronic structure. Care has to be taken that the result is converged with respect to these parameters, at least to the desired level of accuracy. Many molecular conduction results using the above technique now appear in the literature, but no thorough investigation has been published to clarify the effect of these parameters. Here, we address this issue by studying two prototypical systems: an infinite one-dimensional gold chain and Au(111)-XYL-Au(111) where XYL, or 1,4-phenylenedimethanethiol, is a short, thiol-terminated aromatic molecule that easily self-assembles on a gold substrate [9,20,21].

*Corresponding author. Email: mike.ford@uts.edu.au

Molecular Simulation
ISSN 0892-7022 print/ISSN 1029-0435 online © 2007 Taylor & Francis
http://www.tandf.co.uk/journals
DOI: 10.1080/08927020701435811

2. Method

The gold chain and surface adsorption geometries were initially optimized with the SIESTA software package [22], a density functional code employing a linear combination of numerical atomic orbitals as basis functions. The basis set consists of double zeta plus single polarization (DZP) orbitals for each atom. The orbitals have finite extent in space, the cutoff radius being defined by an "energy cutoff" parameter which specifies the excitation energy due to this confinement. This parameter is set to 5 mRy, which corresponds to a cutoff radius for the gold atoms of 3.8 Å for s-orbitals and 2.7 Å for d-orbitals (table 1). The local density approximation (LDA) to the exchange-correlation functional is used, incorporating the self-interaction correction by Perdew and Zunger [23]. Calculations were spin-polarised with the (111) surface represented by a 3×3 atom unit cell, four layers thick. The surface layer is not relaxed during optimization. A reciprocal-space grid with 5×5 k-points in the plane parallel to the surface is constructed according to the method of Monkhorst and Pack [24]. We have previously examined the reliability of this type of calculation against the computational conditions used [25]; the parameters used here correspond to intermediate level I in this previous work and yield adsorption energies that are reliable to better than 0.45 eV. Higher level calculations improve the calculated adsorption energy but do not change adsorption geometries. Here, we are concerned only at locating the minimum adsorption geometry rather than calculating a chemically accurate binding energy. Note that the optimum geometry is determined for the XYL molecule adsorbed through one of the thiol groups to a single gold surface. It is then assumed in the transport calculation, where the molecule spans two surfaces, or electrodes, that the same optimized configuration occurs at both electrodes.

The relaxed geometry is then input into the transport calculation using the ATK package, based on the original TransSIESTA code [26]. This uses the SIESTA method to obtain the electronic structure and calculates transport by using the NEGF method. This code has now been used extensively in the literature, for example, other studies have been undertaken to investigate the effect of different bonding geometries of small organic molecules between gold electrodes on the current–voltage characteristics of the system [27–29].

The molecule with two layers of Au atoms on either side is modeled as the device region, connected on the left and right by semi-infinite electrodes (figure 1(b)). Including two layers in the central region is enough to ensure that the bulk approximation is accurate for the electrodes. A test case calculation with three layers of gold included in the central region yielded no change in the result. In the Au chain calculations, three atoms are included in the device region (figure 1(a)).

We again use the LDA with parametrisation by Perdew and Zunger. In the interest of time, the calculations are done without spin-polarization. This does not introduce an error, since the above (spin-polarized) SIESTA optimisation yielded optimised geometries with a total spin of zero, as expected. The effects of the basis set size describing the gold atoms, the orbital energy cutoff and the number of k-points used in the plane parallel to the surface are investigated within the ATK package. The basis sets used on the atoms within the molecule spanning the electrodes are kept fixed at DZP for each atom. The calculation time is much more sensitive to the basis set size on the gold atoms; this is alternated between DZP ($\zeta_{\mathrm{Au}} = 2$) and single zeta plus polarization ($\zeta_{\mathrm{Au}} = 1$). The orbital confinement parameter E_{c} is varied between 0.02 and 20 mRy. In the case of transport calculations, the determination of the transmission function is a post-electronic structure calculation. The self-consistent electronic structure is characterized by the density matrix, given within the NEGF formalism by Ref. [30]

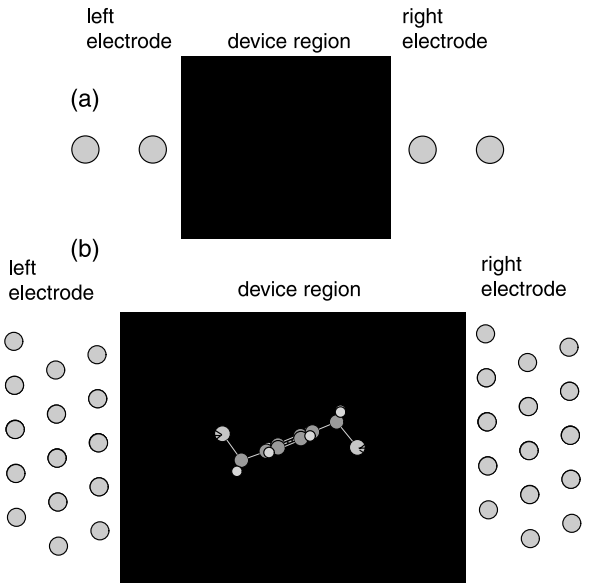

Figure 1. Two probe geometry used for (a) gold chain and (b) Au-XYL-Au calculation.

$$\rho = \frac{1}{2\pi}\int_{-\infty}^{\infty} \mathrm{d}E\left[f(E-\mu_1)G_{\mathrm{d}}\Gamma_1 G_{\mathrm{d}}^{*} + f(E-\mu_2)G_{\mathrm{d}}\Gamma_2 G_{\mathrm{d}}^{*}\right] \tag{1}$$

where $f(E-\mu_{1(2)})$ and $\Gamma_{1(2)}$ are the Fermi functions and coupling matrices of the left (right) electrodes and G_{d} is the device Green's function in the presence of the electrodes.

The electron density and resulting Kohn-Sham operator can be used to evaluate the Hamiltonian at a denser k-point grid, using [22]

$$H_{\mu v}(\vec{k}) = \sum_{\mu' \equiv \mu}\sum_{\nu' \equiv \nu} \mathrm{e}^{i\vec{k}(\vec{R}_{\nu}-\vec{R}_{\mu})}\left\langle \phi_{\mu'}(\vec{r})\middle|\hat{f}^{\mathrm{KS}}\middle|\phi_{\nu'}(\vec{r})\right\rangle \tag{2}$$

where $\mu' \equiv \mu$ indicates all the periodic images of the basis function labeled μ, centered at R_{μ}, without repeating the

SCF at this denser grid. If the electronic structure is converged with respect to the k-point grid used in the SCF cycle, then the lack of self-consistency at the denser grid should not have a large effect. From the Hamiltonian, the Green's function and hence transmission function and current is calculated from Ref. [30]

$$I(V) = \frac{2e}{h}\int_{-\infty}^{\infty} \mathrm{d}E\left[\mathrm{Tr}\left(\Gamma_1 G_\mathrm{d}\Gamma_2 G_\mathrm{d}^*\right)(f(E-\mu_1)-f(E-\mu_2))\right] \tag{3}$$

where the transmission function can be identified as $T(E) = \mathrm{Tr}(\Gamma_1 G_\mathrm{d}\Gamma_2 G_\mathrm{d}^*)$.

For the calculation of the Au-XYL-Au system, we use the same number of grid points N in both the x and y direction. We vary the number of grid points for the self-consistent electronic structure calculation N_E and the transmission function calculation N_T. For the gold chain, only the gamma point is required in either the SCF or transmission function calculation, as there is no periodicity in the transverse direction.

The device region is not periodic and hence no k-point sampling in the direction perpendicular to transport is done in the two-probe calculation. However, for the calculation of the electrodes a large number of k-points, generally 100, is used in this direction to ensure the metallic behaviour of the electrodes.

3. Results and discussion

3.1 Gold chain

Figure 2 shows the current–voltage and conductance-voltage characteristics of a gold chain, calculated with an SZP basis set ($\zeta_\mathrm{Au} = 1$) and $E_\mathrm{c} = 5$ or 10 mRy. The $I(V)$ characteristics seem virtually unaffected, but changing the energy-shift parameter clearly has a larger effect on the conductance. The latter however remains close to the conductance quantum, $G_0 = 2e^2/\mathrm{h} = 77.48\,\mu\mathrm{S}$, as expected for a one-dimensional gold chain [30]. The response of the chain is almost Ohmic, but the conductance decreases slightly at higher voltages. This behaviour has been observed in similar calculations and in experiments [26]. In what follows, we shall refer to the conductance in units of G_0.

The conductance can either be calculated from the difference between successive current evaluations

$$G_\Delta(V) = \frac{I(V+\Delta V) - I(V-\Delta V)}{2\Delta V} \tag{4}$$

or by the analytical derivative of the expression for the current, equation (3), which gives

$$G(V) = \frac{2e^2}{h}\int_{-\infty}^{\infty} \mathrm{d}E{\cdot}T(E)\,\frac{1}{2kT}\left(\frac{t_1}{(1+t_1)^2}+\frac{t_2}{(1+t_2)^2}\right)$$
$$t_1 = \exp\left(\frac{E+eV/2}{kT}\right) \quad t_2 = \exp\left(\frac{E-eV/2}{kT}\right) \tag{5}$$

The conductance given in figure 2(b) is based on equation (4) with $\Delta V = 0.2$ V and $T = 300$ K.

Although equation (5) is exact, it is not necessarily the better option, since discontinuities in the transmission function at energies close to the chemical potentials of the electrodes, can lead to an unreliable conductance value. This is illustrated in figure 3. At 0 V, the transmission function is discontinuous near $E = 0$, where the number of transmission channels changes between one and three. The zero-volt conductance evaluated from equation (5) with $T = 0$ K can therefore be 1 or 3, depending on the exact location of the discontinuity, $E = \varepsilon$. Introducing a finite temperature into equation (5) reduces the sensitivity to ε. The sensitivity is further reduced by using equation (4), where the evaluation of the current integrals occurs over an interval spanning $E = \varepsilon$.

Figure 4 shows the zero-volt conductance of the gold chain calculated from equations (4) and (5) with both $T = 0$ and 300 K. An SZP basis set is used and E_c is varied over a wide range. Some results for a DZP basis set are also shown for comparison.

The conductance is very sensitive to the energy-shift parameter and approaches the expected value of $G = G_0 = 2e^2/\mathrm{h}$ as the basis set orbitals become less confined. When equation (4) is used (figure 4(a)), the conductance is converged at $E_\mathrm{c} = 1$ mRy. Convergence

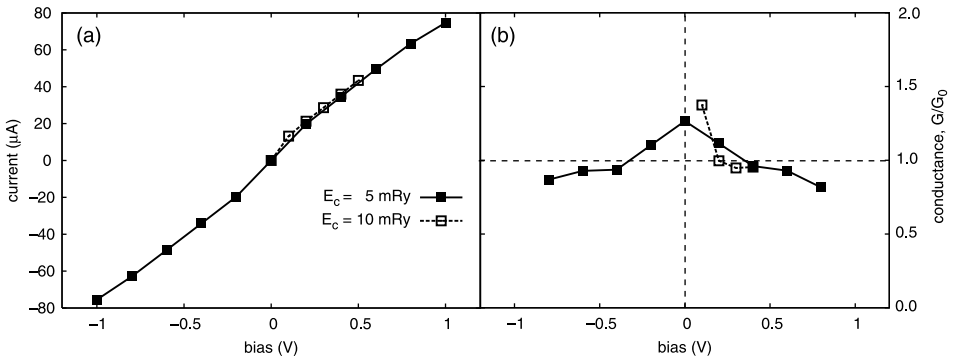

Figure 2. (a) Current–voltage and (b) conductance-voltage characteristics of a gold chain. An SZP basis set is used with the orbital confinement defined through an energy-shift parameter of $E_\mathrm{c} = 5$ or 10 mRy.

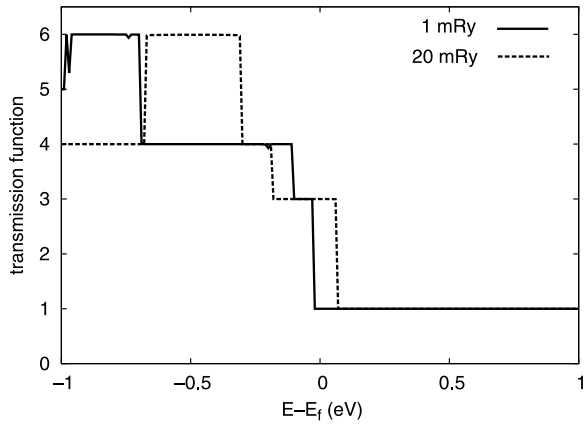

Figure 3. Transmission function for a gold chain with an SZP basis set and energy-shift parameter of $E_c = 1$ or 20 mRy.

with respect to the orbital confinement is faster when $T = 0$ K. Using equation (5) (figure 4(b)), the conductance is converged at $E_c = 1$ mRy when $T = 0$ K, but only at $E_c = 0.1$ mRy when $T = 300$ K. However, at zero-temperature, the convergence is discontinuous and the conductance jumps from G_0 to $3G_0$ between $E_c = 1$ mRy and $E_c = 5$ mRy.

At $E_c = 1$ and 10 mRy the conductance was recalculated with a DZP basis set (hollow data points). These conductance values are invariably very close to their SZP counterparts, the values when $E_c = 1$ mRy and $T = 0$ K being identical.

For accurate conductance results, it is therefore imperative to use an orbital confinement corresponding to an energy-shift parameter of 1 mRy or lower. Table 1 lists the orbital confinement radii corresponding to different values of E_c. Use of a DZP basis set does not provide a significant improvement over SZP and is therefore not recommended, as it implies a significant increase in computational time. For Au, an SZP basis set includes nine orbitals per atom and a DZP basis set 15 orbitals per atom. When using a sufficiently accurate orbital confinement, the zero-temperature conductance is more accurate than the finite-temperature conductance; however, care must be taken when using a less accurate orbital confinement, since a discontinuous transmission function may lead to an incorrect conductance value.

3.2 *Au-XYL-Au*

The potential energy surface (PES) of XYL adsorbed on the Au(111) surface is shown in figure 5. The optimal binding site is slightly offset from the bridge site, towards the fcc site. The binding height is 2.0 Å. The minimum energy position was initially the result of a conjugate gradient (CG) optimisation of the molecule on the surface and the PES was produced by manually varying the binding site and height of the sulphur atom on the surface. This manual scanning of the molecule confirms that the CG result is a global minimum with respect to the sulphur position above the surface.

Figure 6 shows the variation in interaction energy with two independent rotation angles of the molecule on the surface. Firstly, the plane of the phenyl ring was rotated with respect to the surface to make an angle of θ degrees with the surface normal (figure 6(a)). Secondly, the molecule was rotated within the plane of the phenyl ring so that an angle of σ degrees is made between the surface normal and the vector connecting the carbon atoms in the 1 and 4 positions in the ring (figure 6(b)). The inserts in figure 6(a),(b) clarify these rotations. In both cases, the rotations are done about the sulphur atom bound to the surface. In the CG optimised geometry, the rotation angles are $\theta = -21°$ and $\sigma = 0°$. θ and σ are then varied independently with the other angle fixed at the CG optimised value. Manually varying these rotation angles confirms that the CG result is a global minimum with respect to rotation of the molecule on the surface. The minima in figure 6(a),(b) therefore correspond to the same minimum energy structure, shown in figure 6(c).

The interaction energy and optimum geometry is similar to that calculated previously for other thiol-bound molecules; however, the rotation angle may be optimised more reliably by using a *Z*-matrix optimiser [31].

The ATK electronic structure and transport calculations are set up accordingly with the molecule bonded identically to both electrodes.

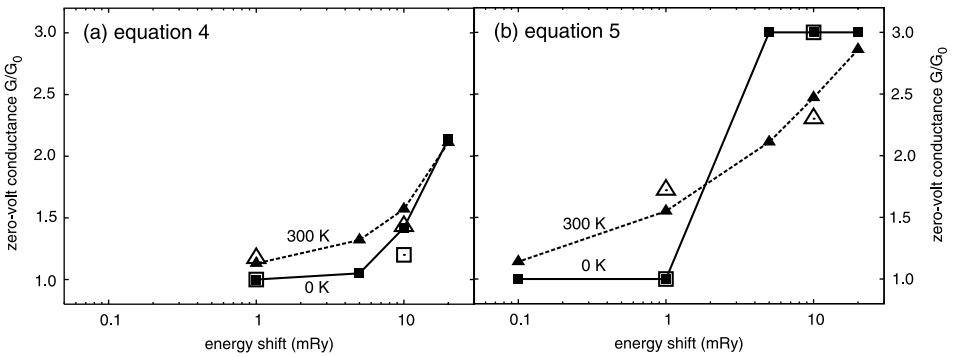

Figure 4. Zero-volt conductance in units of the conductance quantum G_0 at $T = 0$ K and $T = 300$ K, using (a) equation (4) and (b) equation (5). E_c is varied over a wide range for an SZP basis set. The hollow data points at 1 and 10 mRy indicate calculations with a DZP basis set for comparison.

Table 1. Orbital confinement radii corresponding to different values of the energy-shift parameter.

		Energy-shift parameter, E_c (mRy)		
Species	*Orbital*	*5*	*1*	*0.1*
C	2s	2.58	3.07	3.66
C	2p	3.15	3.84	4.82
Au	5d	2.70	3.30	4.03
Au	6s	3.84	4.46	5.44

Firstly, the total energy and the eigenenergies of the highest occupied molecular orbital (HOMO) and lowest unoccupied molecular orbital (LUMO) are calculated with $E_c = 20$ mRy and $\zeta_{Au} = 1$ (SZP), varying N_E between 1 and 13. The results are shown in figure 7. At $N_E = 3$ the total energy has converged to within 1 eV (or 0.01 eV/atom) and the HOMO and LUMO eigenenergies to within 0.005 eV of the limiting values. Here, we have assumed that using a value of $N_e = 13$ gives a converged result.

It is not surprising that the electronic structure is sensitive to *k*-point sampling for this device configuration, which is periodic in two dimensions and therefore possesses dispersive energy bands in *k*-space. However, the total energy and HOMO and LUMO eigenenergies are seen to be well converged at the relatively modest 3×3 *k*-space sampling grid. It should also be noted that more reliable total energy results are obtained by including the gamma point in the *k*-space integration, which in the present code is achieved by using an odd numbered *k*-grid.

For efficiency only the 0 V transmission function was calculated for the XYL system. The zero-volt conductance in what follows was therefore calculated from equation (5), which does not make use of the current at finite voltages. The use of a finite temperature avoids the problem of a discontinuous transmission spectrum described in Section 3.1.

Figure 8 shows the zero-volt conductance of the system calculated from equation (5), using $T = 300$ K, as a function of N_T for various choices of N_E, ζ_{Au} and E_c.

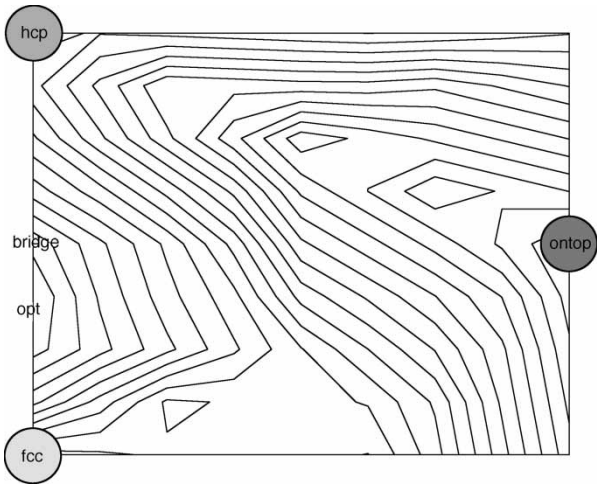

Figure 5. Potential energy surface of XYL adsorbed on Au(111) surface.

Keeping $E_c = 20$ mRy, $\zeta_{Au} = 1$ fixed and varying N_E, N_T (figure 8(a)), the converged value at $N_E = N_T = 13$ is $G = 0.0401\ G_0$. A modest 2×2 *k*-point grid for the SCF calculation seems sufficient for a well converged conductance value and with $N_E = 2$, $N_T = 5$, the zero-volt conductance is converged to within 10% of the limiting value. We use $N_T = 13$, since the calculation of the transmission function occurs post-SCF, and therefore N_T contributes only a small amount to the total computational time. This is quantified in figure 9. The transmission function calculation time is about two orders of magnitude smaller than the electronic structure calculation time and hence the size of the $N_T \times N_T$ grid has negligible effect on the total computation time.

In figure 8(b), E_c, ζ_{Au} and N_E are varied simultaneously. For $N_T = 1$, G changes by up to a factor of three depending on the other parameters, although the errors introduced by ζ_{Au} and E_c appear to cancel. However when convergence is reached with respect to N_T, it seems that the basis set parameters (orbital confinement and basis set size) do not affect the converged value, whereas the *k*-point sampling used for the electronic structure does have an effect.

Finally, we test the convergence of the total energy and zero-volt conductance with respect to the energy-shift parameter, figure 10. We set $\zeta_{Au} = 1$ and $N_E = 1$. We use the gamma point only here in the interest of speed; although the absolute values are therefore not necessarily correct, the convergence behaviour should be unaffected. Taking the values at $E_c = 0.01$ mRy to be converged, the total energy at $E_c = 2$ mRy is converged to within 4 eV (or 0.04 eV/atom) of the limiting value. G evaluated with $N_T = 13$ is converged to within 6% at $E_c = 5$ mRy. However G evaluated with $N_T = 1$, is only well converged at $E_c = 0.5$ mRy, to within 10% of the limiting value. This is consistent with the finding from figure 8(b), i.e. when convergence is reached with respect to N_T, the basis set parameters have less effect on the converged G value.

The best value for the zero-volt conductance of the Au(111)-XYL-Au(111) system presented here is $G = 0.0493\ G_0$, with $N_E = 3$, $N_T = 7$, $E_c = 5$ mRy and $\zeta_{Au} = 2$ (figure 8(b)). This is a factor 82 larger than the experimental measurement of $G = 0.0006\ G_0$ [13]. Discrepancies of this order between calculated and experimental conductances of thiol-bound molecules on gold have been noted before in DFT calculations [32,33].

There is an additional constraint associated with the energy-shift parameter which must be considered in calculations where a vacuum gap is incorporated into the geometry. This would be the case for simulating an STM experiment, or for modeling the effect of moving the molecule away from one electrode [34]. Because the orbitals fall strictly to zero, a sufficiently large orbital confinement radius must be used in order to ensure the gap is spanned by the molecule/electrode orbitals. In other words, a small energy-shift parameter must be used in the transport calculations; the exact value of this parameter will depend upon the geometry. Table 1 gives

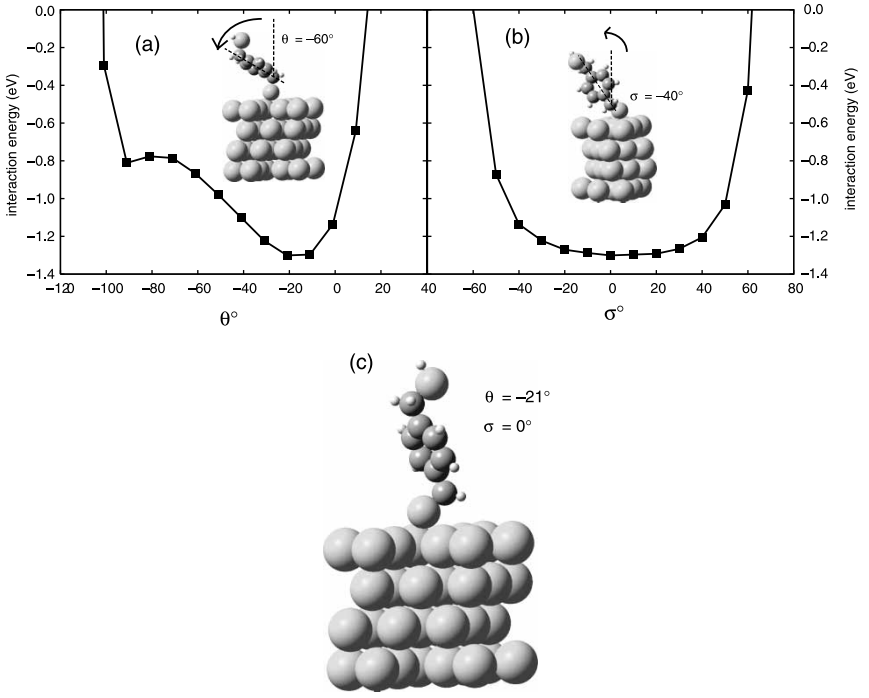

Figure 6. Variation of interaction energy of XYL on Au(111) with rotation of the molecule on the surface: (a) angle θ between phenyl ring and surface normal; (b) angle σ between surface normal and vector joining carbons in the 1 and 4 positions on the ring and (c) minimum energy adsorption geometry ($\theta = -21°$, $\sigma = 0°$).

energy-shifts and the corresponding confined radius for carbon and gold atoms; confinement will vary for different elements even with a common energy-shift. The confinement radii suggest that it may be desirable to use an energy-shift parameter as small as $E_c = 0.1$ mRy when there is a distance of 5–7 Å between molecule and electrode, to ensure significant orbital overlap. This is more accurate than is usually needed to obtain converged adsorption geometries and interaction energies of molecules on surfaces [25]. This is another point that has not been addressed in DFT calculations of transport in the literature. Orbital confinement is not relevant in plane wave codes, but the above discussion is applicable to all codes that use the linear combination of atom orbitals (LCAO) ansatz, where the atom-centred basis functions generally have finite spatial extent.

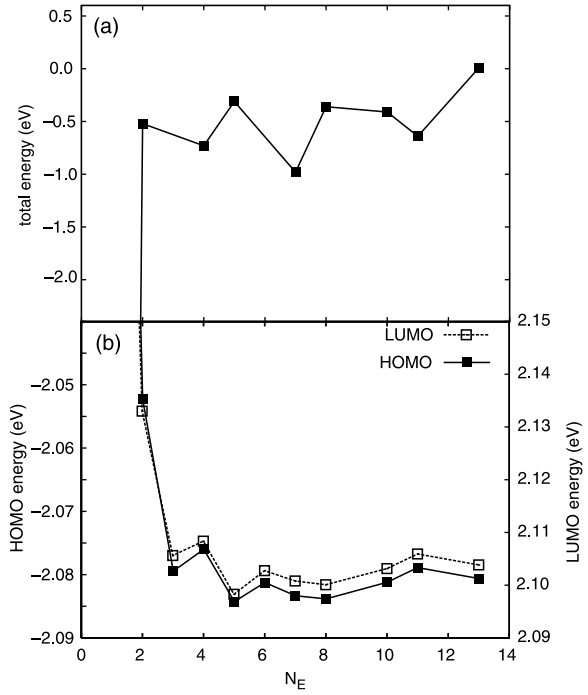

Figure 7. (a) Relative total energy and (b) HOMO and LUMO eigenenergies for different sizes of the k-grid used for the self-consistent electronic structure calculation.

4. Conclusion

In summary, we have conducted a large set of DFT electronic structure and transmission calculations on a gold chain as well as the model Au-XYL-Au system, which is a commonly studied system in the context of single-molecule conductance. For the gold chain, which requires no k-point sampling, we test the effect of altering the basis set parameters on the current and conductance. We find that the $I(V)$ characteristic is relatively insensitive to the basis set, but that the conductance can be highly sensitive to the basis set when the transmission function is discontinuous or rapidly changing. The orbital confinement radius appears to be more important than the number of distinct orbitals per angular momentum channel. This sensitivity can be reduced by applying a finite temperature or by using successive current integration to evaluate the conductance, rather than using the analytical value.

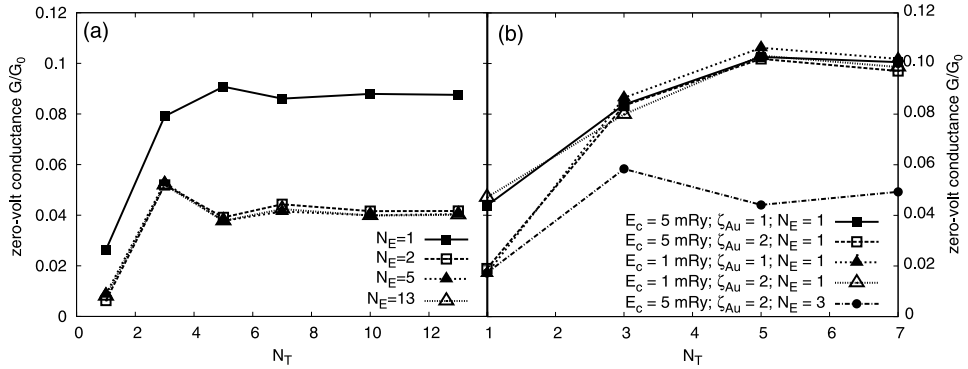

Figure 8. Convergence of the zero-volt conductance for the Au(111)-XYL-Au(111) system calculated with equation (5), while varying the size of the k-point sampling grid used for the transmission function calculation, $N_T \times N_T$ (a) for different SCF k-point sampling grids, $N_E \times N_E$, with $E_c = 20$ mRy, $\zeta_{Au} = 1$; (b) for various combinations of the other parameters, E_c, ζ_{Au} and N_E.

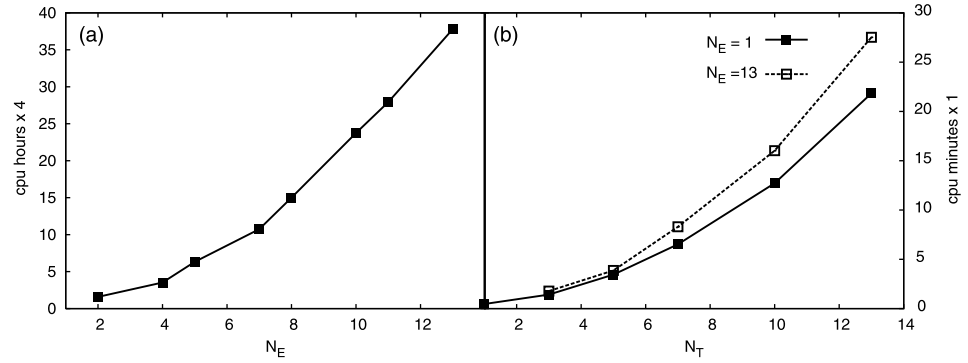

Figure 9. (a) Time taken on four parallel processors to perform the self-consistent electronic structure calculation of the Au-XYL-Au system with various k-grid sizes and $E_c = 20$ mRy, $\zeta_{Au} = 1$; (b) time taken on one processor to calculate the transmission function of the system for various k-grid sizes and $E_c = 20$ mRy, $\zeta_{Au} = 1$.

For the Au-XYL-Au system, we test the variation of the calculated conductance of the system at equilibrium (i.e. 0 volt bias) when certain important variables are changed and find a set of parameters that appear to yield a converged conductance. Including two layers of gold atoms on either side of the device region making up the "extended molecule" is sufficient for a converged result. Changing the basis set size and the orbital confinement and the k-point sampling for both the electronic structure and transmission calculations independently, can change the conductance by typically a factor of three, and even up to a factor of five. We find that the k-point sampling has a more critical effect than the basis set (size and orbital cutoff parameters). The k-point sampling for the electronic structure can be coarser than that of the transmission spectrum calculation. For the Au-XYL-Au system 3 × 3 and 10 × 10 Monkhorst-Pack grids for the two calculations respectively are sufficient. With these grids, using a single zeta plus polarization orbital for gold atoms with the orbital confinement defined by a 5 mRy energy-shift parameter gives a converged conductance. The energy-shift parameter may need to be reduced when considering geometries other than the optimal binding geometry, e.g. with a gap between the molecule and one electrode.

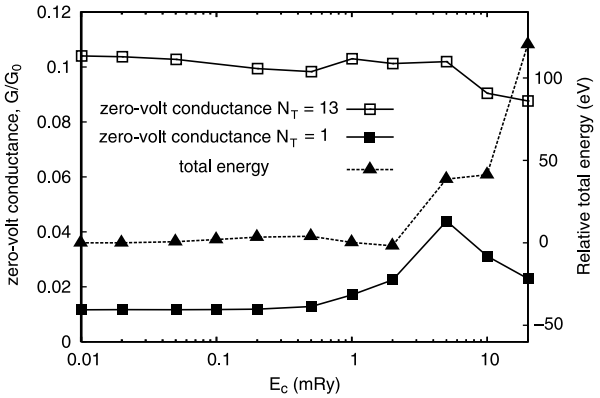

Figure 10. Convergence of total energy (dashed line) and zero-volt conductance (solid lines) with energy-shift parameter. The other parameters are $\zeta_{Au} = 1$ and $N_E = 1$.

Acknowledgements

This work was supported by the Australian Research Council and the University of Technology, Sydney. Computing facilities were provided by the Australian Centre for Computing and Communications (ac3) and the Australian Partnership for Advanced Computing (APAC).

References

[1] M.A. Reed. Molecular-scale electronics. *Proc. IEEE*, **87**, 652 (1999).

[2] D.K. James, J.M. Tour. Electrical measurements in molecular electronics. *Chem. Mater.*, **16**, 4423 (2004).

[3] Y.Q. Xue, M.A. Ratner. Theoretical principles of single-molecule electronics: a chemical and mesoscopic view. *Int. J. Quantum Chem.*, **102**, 911 (2005).

[4] A. Nitzan, M.A. Ratner. Electron transport in molecular wire junctions. *Science*, **300**, 1384 (2003).

[5] J.C. Love, L.A. Estroff, J.K. Kriebel, R.G. Nuzzo, G.M. Whitesides. Self-assembled monolayers of thiolates on metals as a form of nanotechnology. *Chem. Rev.*, **105**, 1103 (2005).

[6] R.P. Andres, J.D. Bielefeld, J.I. Henderson, D.B. Janes, V.R. Kolagunta, C.P. Kubiak, W.J. Mahoney, R.G. Osifchin. Self-assembly of a two-dimensional superlattice of molecularly linked metal clusters. *Science*, **273**, 1690 (1996).

[7] L.A. Bumm, J.J. Arnold, M.T. Cygan, T.D. Dunbar, T.P. Burgin, L. Jones, D.L. Allara, J.M. Tour, P.S. Weiss. Are single molecular wires conducting? *Science*, **271**, 1705 (1996).

[8] S. Datta, W.D. Tian, S.H. Hong, R. Reifenberger, J.I. Henderson, C.P. Kubiak. Current–voltage characteristics of self-assembled monolayers by scanning tunneling microscopy. *Phys. Rev. Lett.*, **79**, 2530 (1997).

[9] M. Dorogi, J. Gomez, R. Osifchin, R.P. Andres, R. Reifenberger. Room-temperature Coulomb-blockade from a self-assembled molecular nanostructure. *Phys. Rev. B*, **52**, 9071 (1995).

[10] T. Ishida, W. Mizutani, N. Choi, U. Akiba, M. Fujihira, H. Tokumoto. Structural effects on electrical conduction of conjugated molecules studied by scanning tunneling microscopy. *J. Phys. Chem. B*, **104**, 11680 (2000).

[11] K. Moth-Poulsen, L. Patrone, N. Stuhr-Hansen, J.B. Christensen, J.P. Bourgoin, T. Bjornholm. Probing the effects of conjugation path on the electronic transmission through single molecules using scanning tunneling microscopy. *Nano Lett.*, **5**, 783 (2005).

[12] J.J.W.M. Rosink, M.A. Blauw, L.J. Geerligs, E. van der Drift, S. Radelaar. Tunneling spectroscopy study and modeling of electron transport in small conjugated azomethine molecules. *Phys. Rev. B*, **62**, 10459 (2000).

[13] X.Y. Xiao, B.Q. Xu, N.J. Tao. Measurement of single molecule conductance: benzenedithiol and benzenedimethanethiol. *Nano Lett.*, **4**, 267 (2004).

[14] B.Q. Xu, N.J.J. Tao. Measurement of single-molecule resistance by repeated formation of molecular junctions. *Science*, **301**, 1221 (2003).

[15] T. Bohler, J. Grebing, A. Mayer-Gindner, H.V. Lohneysen, E. Scheer. Mechanically controllable break-junctions for use as electrodes for molecular electronics. *Nanotechnology*, **15**, S465 (2004).

[16] M.A. Reed, C. Zhou, C.J. Muller, T.P. Burgin, J.M. Tour. Conductance of a molecular junction. *Science*, **278**, 252 (1997).

[17] J. Reichert, R. Ochs, D. Beckmann, H.B. Weber, M. Mayor, H. von Lohneysen. Driving current through single organic molecules. *Phys. Rev. Lett.*, **88**, 176804 (2002).

[18] X.D. Cui, A. Primak, X. Zarate, J. Tomfohr, O.F. Sankey, A.L. Moore, T.A. Moore, D. Gust, G. Harris, S.M. Lindsay. Reproducible measurement of single-molecule conductivity. *Science*, **294**, 571 (2001).

[19] S.M. Lindsay, M.A. Ratner. Molecular transport junctions: clearing mists. *Adv. Mater.*, **19**, 23 (2007).

[20] J.I. Henderson, S. Feng, G.M. Ferrence, T. Bein, C.P. Kubiak. Self-assembled monolayers of dithiols, diisocyanides, and isocyanothiols on gold: 'Chemically sticky' surfaces for covalent attachment of metal clusters and studies of interfacial electron transfer. *Inorg. Chim. Acta*, **242**, 115 (1996).

[21] H.M. Zareie, A.M. McDonagh, J. Edgar, M.J. Ford, M.B. Cortie, M.R. Phillips. Controlled assembly of 1,4-phenylenedimethanethiol molecular nanostructures. *Chem. Mater.*, **18**, 2376 (2006).

[22] J.M. Soler, E. Artacho, J.D. Gale, A. Garcia, J. Junquera, P. Ordejon, D. Sanchez-Portal. The SIESTA method for *ab initio* order-N materials simulation. *J. Phys.: Condens. Matter*, **14**, 2745 (2002).

[23] J.P. Perdew, A. Zunger. Self-interaction correction to density-functional approximations for many-electron systems. *Phys. Rev. B*, **23**, 5048 (1981).

[24] H.J. Monkhorst, J.D. Pack. Special points for Brillouin-zone integrations. *Phys. Rev. B*, **13**, 5188 (1976).

[25] M.J. Ford, R.C. Hoft, A. McDonagh. First principles theoretical prediction of a new class of self-assembled monolayer: ethynylbenzenes on gold. *J. Phys. Chem. B*, **109**, 20387 (2005).

[26] M. Brandbyge, J.L. Mozos, P. Ordejon, J. Taylor, K. Stokbro. Density-functional method for nonequilibrium electron transport. *Phys. Rev. B*, **65**, 165401 (2002).

[27] K.H. Muller. Effect of the atomic configuration of gold electrodes on the electrical conduction of alkanedithiol molecules. *Phys. Rev. B*, **73**, 045403 (2006).

[28] Y.B. Hu, Y. Zhu, H.J. Gao, H. Guo. Conductance of an ensemble of molecular wires: a statistical analysis. *Phys. Rev. Lett.*, **95**, 156803 (2005).

[29] H. Basch, R. Cohen, M.A. Ratner. Interface geometry and molecular junction conductance: geometric fluctuation and stochastic switching. *Nano Lett.*, **5**, 1668 (2005).

[30] S. Datta. *Quantum Transport: Atom to Transistor*, Cambridge University Press, Cambridge (2005).

[31] M.J. Ford, R.C. Hoft, J.D. Gale. Adsorption and dimerisation of thiol molecules on Au(111) using a *Z*-matrix approach in density functional theory. *Mol. Sim.*, **32**, 1219 (2006).

[32] M. Di Ventra, S.T. Pantelides, N.D. Lang. First-principles calculation of transport properties of a molecular device. *Phys. Rev. Lett.*, **84**, 979 (2000).

[33] K. Stokbro, J. Taylor, M. Brandbyge, J.L. Mozos, P. Ordejon. Theoretical study of the nonlinear conductance of Di-thiol benzene coupled to Au(111) surfaces via thiol and thiolate bonds. *Comp. Mater. Sci.*, **27**, 151 (2003).

[34] R.C. Hoft, M. Ford, M.B. Cortie. Prediction of increased tunneling current by bond length stretch in molecular break junctions. *Chem. Phys. Lett.*, **429**, 503 (2006).